



Effective Mode Shapes of Viaducts Subjected to High-speed Train

Hızlı Tren Geçişine Maruz Kalan Viyadüklerin Etkin Mod Şekilleri

Salih Demirtaş^{1*} and Hasan Öztürk²

¹ Erzincan Binali Yıldırım Üniversitesi, Mühendislik Fakültesi, Makine Mühendisliği Bölümü, Erzincan, TÜRKİYE

² Dokuz Eylül Üniversitesi Mühendislik Fakültesi Makina Mühendisliği Bölümü, İzmir, TÜRKİYE

Sorumlu Yazar / Corresponding Author *: salih.demirtas@deu.edu.tr

Geliş Tarihi / Received: 10.03.2020

Kabul Tarihi / Accepted: 16.07.2020

Araştırma Makalesi/Research Article

DOI:10.21205/deufmd.2021236726

Atıf şekli/How to cite: DEMİRTAŞ, S., ÖZTÜRK, H. (2021). Effective Mode Shapes of Viaducts Subjected to High-speed Train. DEUFMD, 23(67), 295-307

Abstract

The high-speed railways require more viaducts than conventional railways. The dynamic interaction effect between train and viaduct are important issue due to the risk of derailment, structural safety and deterioration of the passenger comfort. In this study, viaduct is modelled as a multi-bay frame. The multi-bay frame is modelled by finite element method. The train is idealized as a two-axle system with 4 degrees of freedom. The equations of motions of the coupled vehicle-structure system are determined via generalized Lagrange's equation. The Wilson-theta time integration method is employed to determine the dynamic response of the system. The effective mode shapes are investigated using 3D frequency-velocity-amplitude graphs. The resonant response has been determined at first and second modes of 1 and 2-bay frames.

Keywords: viaduct, mode shape, finite element method, Wilson-theta method, train

Öz

Yüksek hızlı demiryolları, geleneksel demiryollarından daha fazla viyadük gerektirir. Tren ve viyadük arasındaki dinamik etkileşim etkisi, raydan çıkma, yapısal güvenlik ve yolcu konforunun bozulması nedeniyle önemli bir konudur. Bu çalışmada viyadük çok bölmeli bir çerçeve olarak düşünülmüştür. Çok bölmeli çerçeve sonlu elemanlar yöntemi ile modellenmiştir. Tren, 4 serbestlik dereceli iki akslı sistem olarak idealize edilmiştir. Birleştirilmiş araç-yapı sisteminin hareket denklemleri genelleştirilmiş Lagrange denklemi ile belirlenmiştir. Sistemin dinamik yanıtını belirlemek için Wilson-teta zaman integrasyonu yöntemi kullanılmıştır. Etkin mod şekilleri, 3D frekans-hız-genlik grafikleri kullanılarak araştırılmıştır. 1 ve 2 bölmeli çerçevelerin birinci ve ikinci modlarının, yapının rezonans cevabında baskın olduğu belirlenmiştir.

Anahtar Kelimeler: viyadük, mod şekli, sonlu elemanlar metodu, Wilson-theta metodu, tren

1.Introduction

Dynamic responses of structures, such as bridges, viaducts, under the action of train loads have seen considerable interests in the field of civil engineering. With the development of high-speed trains, dynamic analysis of railway bridges has become important.

Viaducts are used mainly for the purpose of connecting two points of the terrain which are similar in height in order to carry mostly rail and road traffic. Su et al. studied the dynamic responses of a viaduct subject to high speed train[1]. Lou et al. have been presented modal coordinate formulation for analysing the dynamic interaction between a simply supported bridge and a moving train. Train is modelled as two-stage suspension vehicles with 10 DOF. Bridge is modelled as a uniform simply supported beam, based on Euler-Bernoulli beam theory. Rayleigh damping is assumed for the bridge[2]. In the literature, the dynamic behavior of structures subjected to four-axle two-bogie train with 10 unconstrained degrees of freedom is investigated by authors [3-7]. Other train models have been studied, such as those 2-axle 6 DOF by [8] , 4 DOF by [9] ; moving suspension mass model [10].

The resonant response of the train-bridge system is of particular interest due to the structural safety of the bridge, risk of derailment and deterioration of passenger comfort. Resonance occurs if one of the dominant frequencies of the train load equals to a multiple

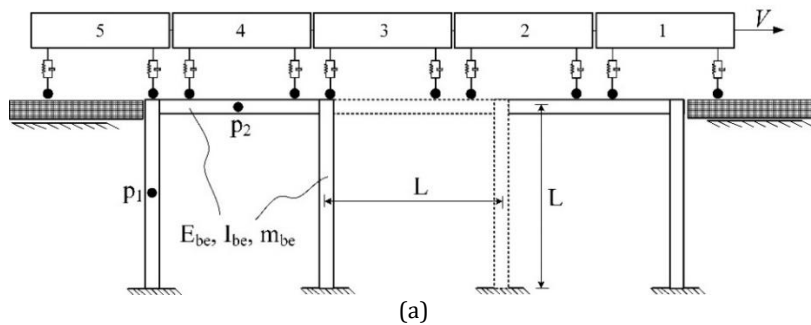
of one of the natural frequencies of the structure. The lower natural frequencies of the structures used in high speed train lines means that the structure can resonate at a smaller speed value. 3D frequency-speed-amplitude graphs are plotted for this purpose. It was determined whether the peaks in this graph force the structure under resonance conditions.

The study on the dynamic analyses of the viaduct-like structures modelled as a multi-bay frame under the effects of moving vehicles are rare. There are not many studies on this subject in the existing literature. In this study, the viaduct is considered to be modelled as a multi-bay frame. The multi-bay frame, based on Bernoulli-Euler beam theory, has the boundary conditions of zero horizontal and vertical displacements and zero rotations at the bases of columns. Also, the train is idealized as a 2-axle system with 4 DOF.

2. Theory

2.1. System description

The problem to be dealt with in the present study is a multi-bay frame subjected to moving train, shown in Fig. 1. Bernoulli-Euler beams forming the frame have beam (column) length L , elastic modulus E_{be} , area moment of inertia I_{be} , mass per unit length m_{be} . Points p_1 and p_2 are corresponding to midpoint of the column and top beam, respectively.



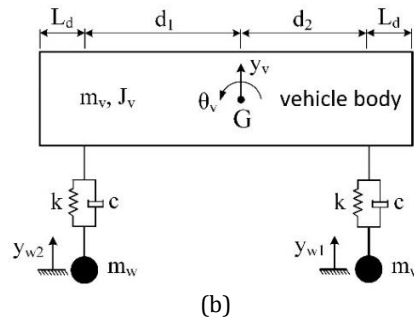


Figure 1. Vehicle-structure system: (a)structure model (b) vehicle model

The vehicle considered to be as a model of the train consist of suspension system having stiffness k and damping c . The m_w and m_v are the respective, the mass of a wheelset and mass of a vehicle body. J_v is the corresponding mass moment of inertia of a bogie and vehicle body. L_d is the longitudinal distance between the centre of gravity of bogie and nearest side of vehicle body. d_1 (d_2) is the horizontal distance between the centre of gravity of vehicle body and of rear (front) bogie. G is the center of gravity of the

2.2. Vehicle-structure interaction dynamics

In this study, a two-axle vehicle travelling at a uniform speed V on a frame was investigated, shown in Fig. 2. $x_i(t)$ ($i=1,2$) is the contact point between the frame and i th axle measured from the left end of the top beam. It is assumed that two wheelsets and frame are in contact with elements e_i ($i=1,2$) at a time t . $q_1^{e_i}$ and $q_4^{e_i}$ ($i=1,2$) denote the vertical displacements at nodes of element e_i .

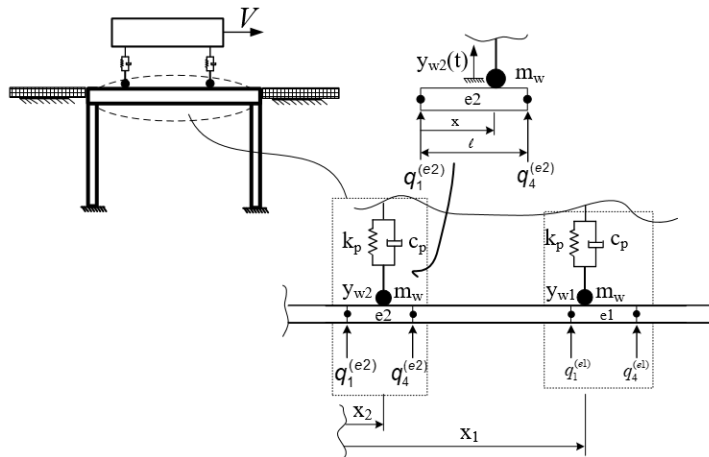


Figure 2. A vehicle travelling on a 1-bay frame

vehicle body.

As seen Fig. 1 (b), $y_{wi}(t)$ ($i=1,2$) denote the vertical displacement of the i th wheelset. y_v is vertical displacement of the vehicle body. Also, θ_v is rotation of vehicle body. The vehicle has four unconstrained degrees of freedom. It is assumed that the upward vertical displacements are taken as positive and that they are measured from the respective static equilibrium positions.

The equation of motion of the frame and vehicle are derived from the following generalized Lagrange's equation:

$$\frac{d}{dt} \left(\frac{\partial T}{\partial \dot{u}_k} \right) - \frac{\partial T}{\partial u_k} + \frac{\partial \bar{V}}{\partial u_k} + \frac{\partial D}{\partial \dot{u}_k} = f_k, \quad k=1,2,\dots \quad (1)$$

The kinetic, potential energy and dissipation function of the integrated system can be written as

$$T = \frac{1}{2} \sum_{i=1}^2 m_{wi} \dot{y}_{wi}^2 + \frac{1}{2} J_v \dot{\theta}_v^2 + \frac{1}{2} m_v \dot{y}_v^2 + \dot{\mathbf{q}}_f^T \mathbf{M}_f \dot{\mathbf{q}}_f$$

$$\bar{V} = \frac{1}{2} k_s \left[(y_v + d_2 \theta_v - y_{w1})^2 + (y_v - d_1 \theta_v - y_{w2})^2 \right] \quad (2)$$

$$D = \frac{1}{2} c_s \left[(\dot{y}_v + d_2 \dot{\theta}_v - \dot{y}_{w1})^2 + (\dot{y}_v - d_1 \dot{\theta}_v - \dot{y}_{w2})^2 \right] + \dot{\mathbf{q}}_f^T \mathbf{K}_f \dot{\mathbf{q}}_f$$

where \mathbf{M}_f and \mathbf{K}_f are the mass and stiffness matrices of the frame[11]. \mathbf{q}_f and $\dot{\mathbf{q}}_f$ are the vectors of nodal displacement and velocity of the frame, respectively.

The total number of degrees of freedom of vehicle is four. It is assumed that the wheels always keep in contact with the structure. This indicates that the structure and wheelsets do not move independently of each other. Therefore, the vertical displacement/velocity of each wheelset is equal to the vertical displacement/velocity of the point where it contacts the frame:

$$y_{wi} = N_1(\xi) q_1^{ei} + N_2(\xi) q_4^{ei}, \quad i = 1, 2, 3, 4$$

$$\dot{y}_{wi} = N_1(\xi) \dot{q}_1^{ei} + VN_1(\xi)_{,x} q_1^{ei} + N_2(\xi) \dot{q}_4^{ei} + VN_2(\xi)_{,x} q_4^{ei}, \quad i = 1, 2, 3, 4 \quad (3)$$

where the derivative of a function $f(x)$ with respect to x is denoted by $f(x)_{,x}$, $\xi = x/l$ (see Fig. 3) and N_i ($i=1,2$) are interpolation functions:

$$N_1 = 1 - 3\xi^2 + 2\xi^3, \quad N_2 = 3\xi^2 - 2\xi^3 \quad (4)$$

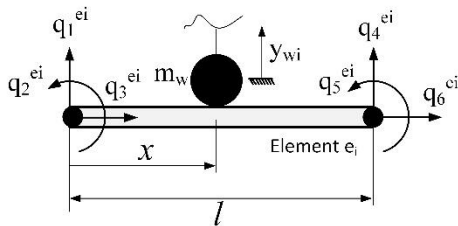


Figure 3. Nodal degrees of freedom of the beam element e_i

Nodal degrees of freedom of the element e_i is shown in Fig. 3 and nodal displacement vector are as follows:

$$\mathbf{q}_f^{e_i} = \{q_1^{e_i}, q_2^{e_i}, q_3^{e_i}, q_4^{e_i}, q_5^{e_i}, q_6^{e_i}\}, \quad i = 1, 2, 3, 4 \quad (5)$$

and displacement vector of vehicle and combined vehicle-structure system are following:

$$\mathbf{q}_v = \{y_{b1}, y_{b2}, y_v, \theta_{b1}, \theta_{b2}, \theta_v\} \quad (6)$$

$$\mathbf{U} = \{u_1, u_2, u_3, \dots, u_N, y_{b1}, y_{b2}, y_v, \theta_{b1}, \theta_{b2}, \theta_v\}$$

After some algebraic manipulations, the following equations of motion for the system can be obtained

$$\begin{bmatrix} \mathbf{M}_f + \sum_{i=1}^2 \mathbf{M}_{fv}^i & \mathbf{0} \\ \mathbf{0} & \mathbf{M}_v \end{bmatrix} \begin{Bmatrix} \ddot{\mathbf{q}}_f \\ \ddot{\mathbf{q}}_v \end{Bmatrix} + \begin{bmatrix} \sum_{i=1}^2 \mathbf{C}_{fv}^i & \bar{\mathbf{C}}_{vf} \\ \bar{\mathbf{C}}_{vf}^T & \mathbf{C}_v \end{bmatrix} \begin{Bmatrix} \dot{\mathbf{q}}_f \\ \dot{\mathbf{q}}_v \end{Bmatrix} + \begin{bmatrix} \mathbf{K}_f + \sum_{i=1}^2 \mathbf{K}_{fv}^i & \bar{\mathbf{K}}_{vf} \\ \bar{\mathbf{K}}_{vf}^T & \mathbf{K}_v \end{bmatrix} \begin{Bmatrix} \mathbf{q}_f \\ \mathbf{q}_v \end{Bmatrix} = \begin{Bmatrix} \mathbf{f} \\ \mathbf{0} \end{Bmatrix} \quad (7)$$

(7) where the subscripts v and f represent the vehicle and the frame, respectively. The index vf (or fv) in matrices is the result of the interaction between the structure and the vehicle. \mathbf{M}_{fv} and \mathbf{K}_{fv} are the $N \times N$ matrices and $\bar{\mathbf{C}}_{vf}$ and $\bar{\mathbf{K}}_{vf}$ are $N \times 2$ matrices. The non-zero columns of these matrices are given in appendix.

When the vehicle runs on the structure, matrices with double subscript and the vector of f are always changing. As a consequence of this, Eq. (7) becomes a second-order differential equation with variable coefficients. Those time-variable coefficients should be updated every time interval before numerical integration process apply. Eq. (7) can then be solved by using the Wilson-theta time integration scheme with $\theta = 1.4$ [12].

2.2.1. Validation

A simply supported beam subjected to a single vehicle is considered. The example model has

Table 1: Parameters of vehicle, and of multi-bay frame

Description	Notation	Unit	Value
Vehicle			
Mass of the vehicle body	m_v	kg	48e3
Mass of a wheelset	m_w	kg	5e3
Mass moment of inertia of vehicle body	J_v	kg	2500e3
Horizontal distance between the centre of gravity of car body and of rear suspension system	d_1	m	9
Horizontal distance between the centre of gravity of car body and of front suspension system	d_2	m	9
Longitudinal distance between the centre of gravity of suspension system and nearest side of vehicle body	L_d	m	3.5
Stiffness of suspension system	k	N/m	1500e3
Damping of suspension system	c	N.s/m	85e3
Multi-bay frame			
Beam/column length of frame	L	m	30
Moment of inertia	I_{be}	m^4	2.9
Mass per unit length	m_{be}	kg/m	1.2e4
Young's modulus	E_{be}	Pa	2.87 e9

been studied by [13]. Fig. 4 show good agreement between present model and model in Ref. [13].

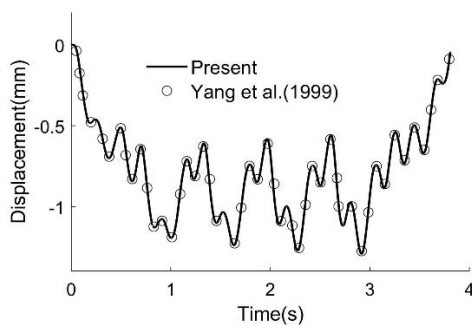


Figure 4: Vertical displacement of the midpoint of the beam

3. Dominant Mode Shapes of the Multi-bay frame

All the parameters which is used in subsequent computations have been given in Table 1. The values of physical properties are taken from [13].

3.1. Modal Analysis of the Multi-bay Frame

The first few natural frequencies are determined using both ANSYS and the developed MATLAB programs (present work). The beams and columns are modelled using BEAM54 element.

ANSYS BEAM54 is used because it has the same nodal degrees of freedom with the model developed by present work. Element size is taken as 5m to generate same finite element

Table 2: The first few natural frequencies (f) of i-bay frame (i=1,2)

f(Hz)	1-bay frame		2-bay frame	
	Present work	ANSYS	Present work	ANSYS
f ₁	0.4714	0.47135	0.4370	0.4370
f ₂	1.8477	1.8442	1.7933	1.7898
f ₃	3.0356	3.0267	2.2309	2.2265
f ₄			3.0555	3.0469

mesh those of the developed model. Table 2 shows the natural frequencies of i-bay frame(i=1,2).

The mode shapes corresponding to natural frequencies given in Table 2 are plotted. The first modes of the structures shown in Figs. 5 are related to the first bending modes of the columns forming the frame.

The vertical displacements of the top beam are negligible in these modes. Due to train travelled on the top beam, it can be expected that mode shapes which vertical displacements of the top beam are effective are important on resonance response. Therefore, the 2nd and 4th modes of the 1-bay frame and the 2nd and 3rd modes of the 2-bay frame may be effective in resonance response of the structure.

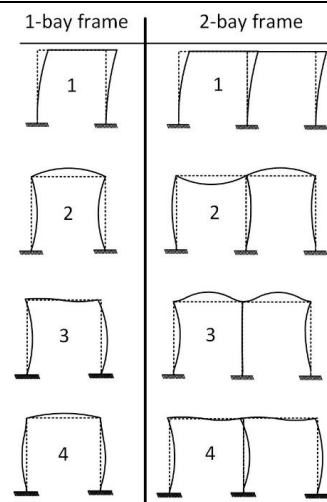


Figure 5: Mode shapes of i-bay frame(i=1,2) corresponding to the natural frequencies listed in Table 2

3.2. Velocity-Frequency-Amplitude Graphs

3D relationship of velocity-frequency-amplitude graphs was plotted with respect to horizontal displacements of the point p₁ and vertical displacements of the point p₂ (see Fig. 1(a)). The displacement-time history curves of the i-bay frame (i=1,2) was first determined at each velocity (V = 1,2, ..., 100). Then, frequency responses were obtained by applying the Fourier transform to free vibrations. It should be noted that the number of vehicles is taken as 5 when plotting 3D graphics. However, in order to better visualize resonance, the number of vehicles in the displacement-time history curves was selected as 10.

3.2. 1. 1-bay frame

The 3D views of the velocity-frequency-amplitude plot is illustrated in Figs. 6. Three frequency peaks occur in Fig. 6(a). The resonance vibration may occur at those critical velocities corresponding to the peaks. Velocities and frequencies can be read as f₁ =0.47 Hz, V=12 m/s; f₂ =1.847 Hz, V=47 m/s; and f₃ =3.04 Hz, V=77 m/s.

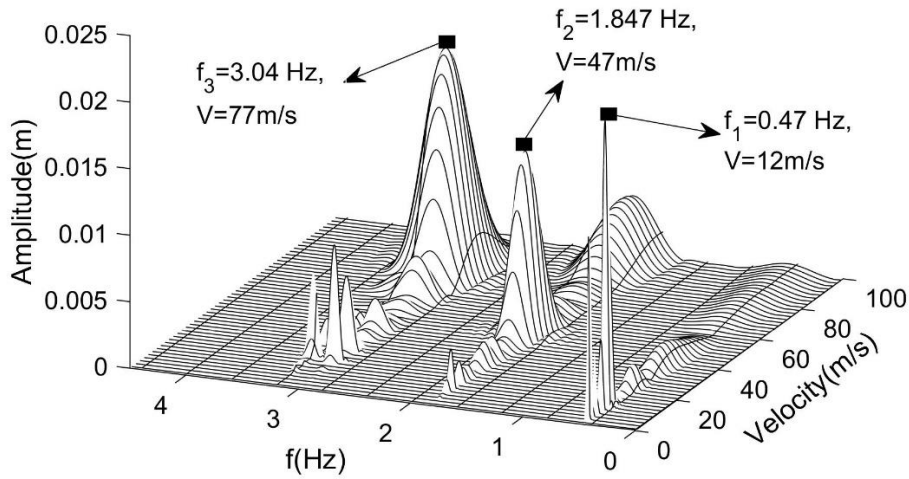
It is shown in Fig. 6(b) that there is a peak amplitude and its value can be extracted as f₂=1.847 Hz, V=47 m/s.

The displacement-time history curves for velocities determined from Fig. 6 are plotted, as

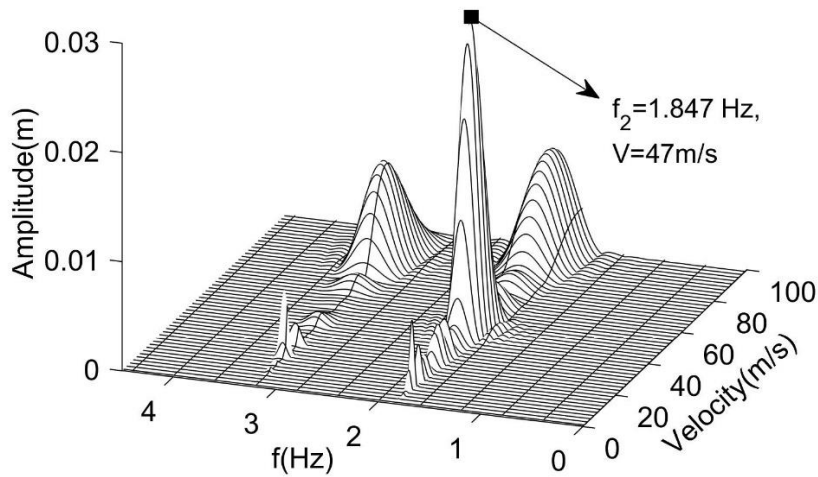
seen in Figs. 7. Fig. 7 (a1) shows resonance behaviour in horizontal direction. From Figs.7 (a1) and (b1), the velocity $V=12$ m/s has excited the first mode of vibrations.

The speed of train having velocity of $V=47$ m/s is excited the 2nd mode of vibrations. It would be the first dominant natural frequency which the

resonant responses are encountered not only in the horizontal but also in the vertical direction. The maximum amplitude in the vertical direction has been determined when comparing with Figs7 (b1) and (b3). It clear that resonance response cannot be appear in 3rd mode (Figs. 7 (a3), (b3)).



(a)



(b)

Figure 6: 3D velocity-frequency-amplitude graphs for 1-bay frame: (a) horizontal displacement of the point 1, (b) vertical displacement of the point 2

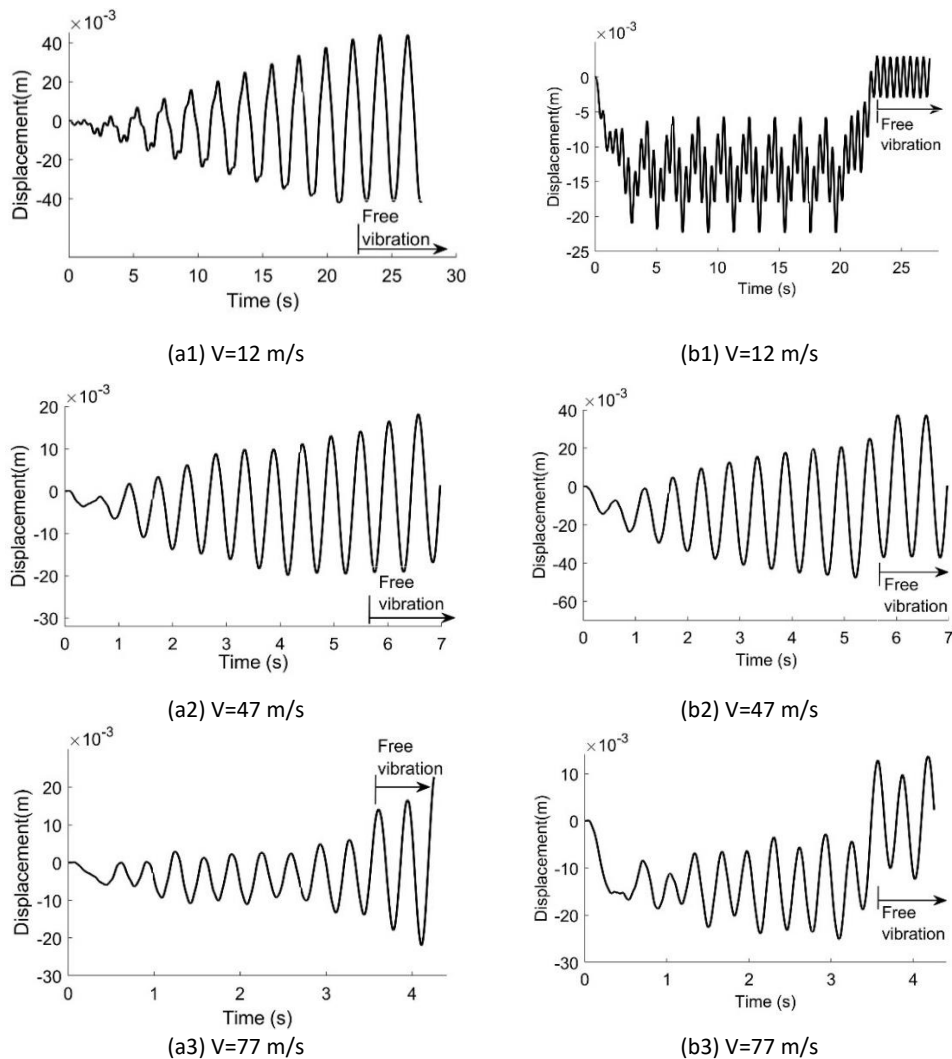


Figure 7: Figs. (ai) and (bi) ($i=1,2,3$) are corresponding to displacements at points p1 in the horizontal direction and p2 in the vertical directions, respectively

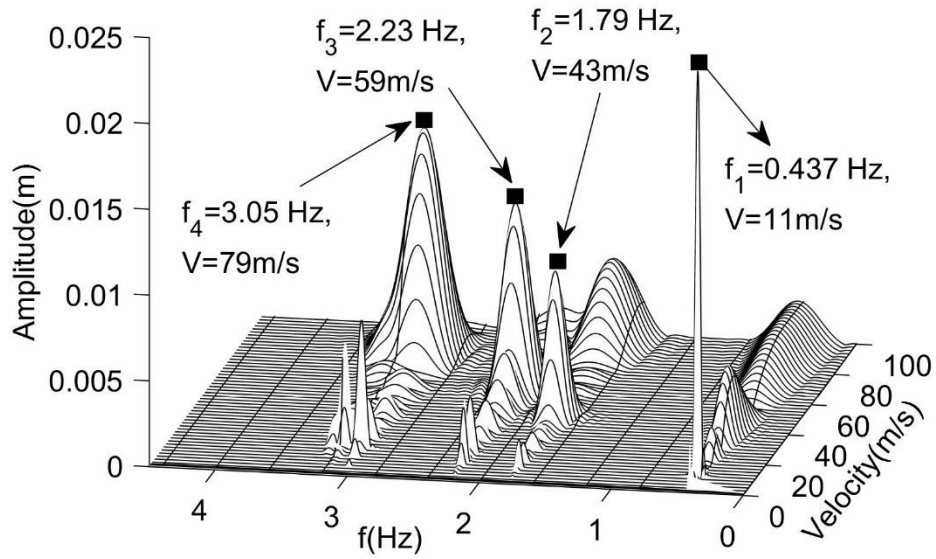
3.2. 1. 2-bay frame

Figs. 8 shows the four possible resonance peaks. The velocity and frequency values corresponding to these peak amplitudes are as follows: $f_1=0.437$ Hz, $V=11$ m/s; $f_2=1.79$ Hz, $V=42$ m/s; $f_3=2.23$ Hz, $V=57$ m/s and $f_4=3.05$ Hz, $V=74$ m/s. It is clear that the largest amplitude occurs when $f_1=0.437$ Hz, $V=11$ m/s.

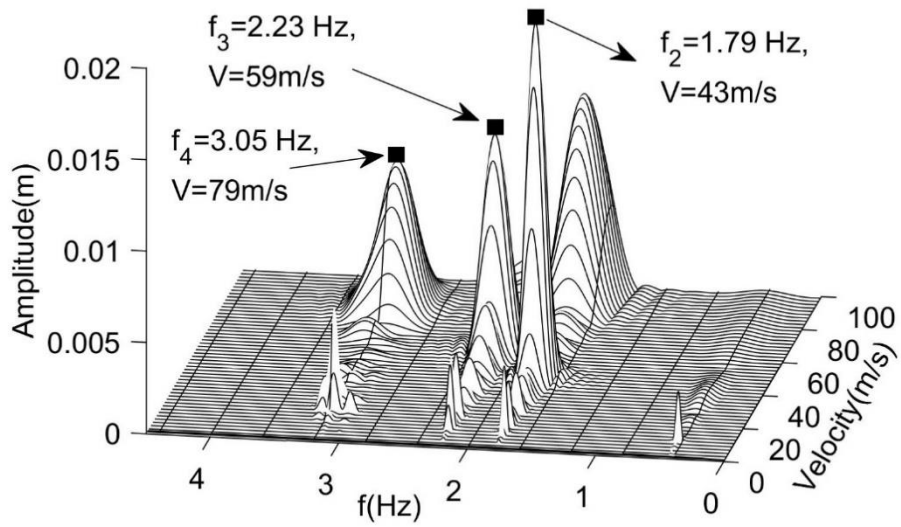
It is seen in Fig. 8 (b) that mode 2 is effective in vibrations in the vertical directions of the structure within the speed range of interest. The

amplitudes peaks in the figure are: $f_2=1.79$ Hz, $V=42$ m/s and $f_3=2.23$ Hz, $V=57$ m/s.

Fig. 9 (a1) shows the resonant response in horizontal direction. This means that the first mode can be the dominant mode in the vibrations of point p1 in the horizontal direction. The resonance responses in both the vertical and the horizontal directions are illustrated in Figs. 9 (a2) and (b2). Those figures are associated with the 2nd mode. In Figs. 9(a3), (b3), (a4) and (b4), the resonant response does not occur at velocities of 57 m/s and 74 m/s.



(a)



(b)

Figure 8: 3D velocity-frequency-amplitude graphs for 2-bay frame: (a) horizontal displacement of the point 1, (b) vertical displacement of the point 2

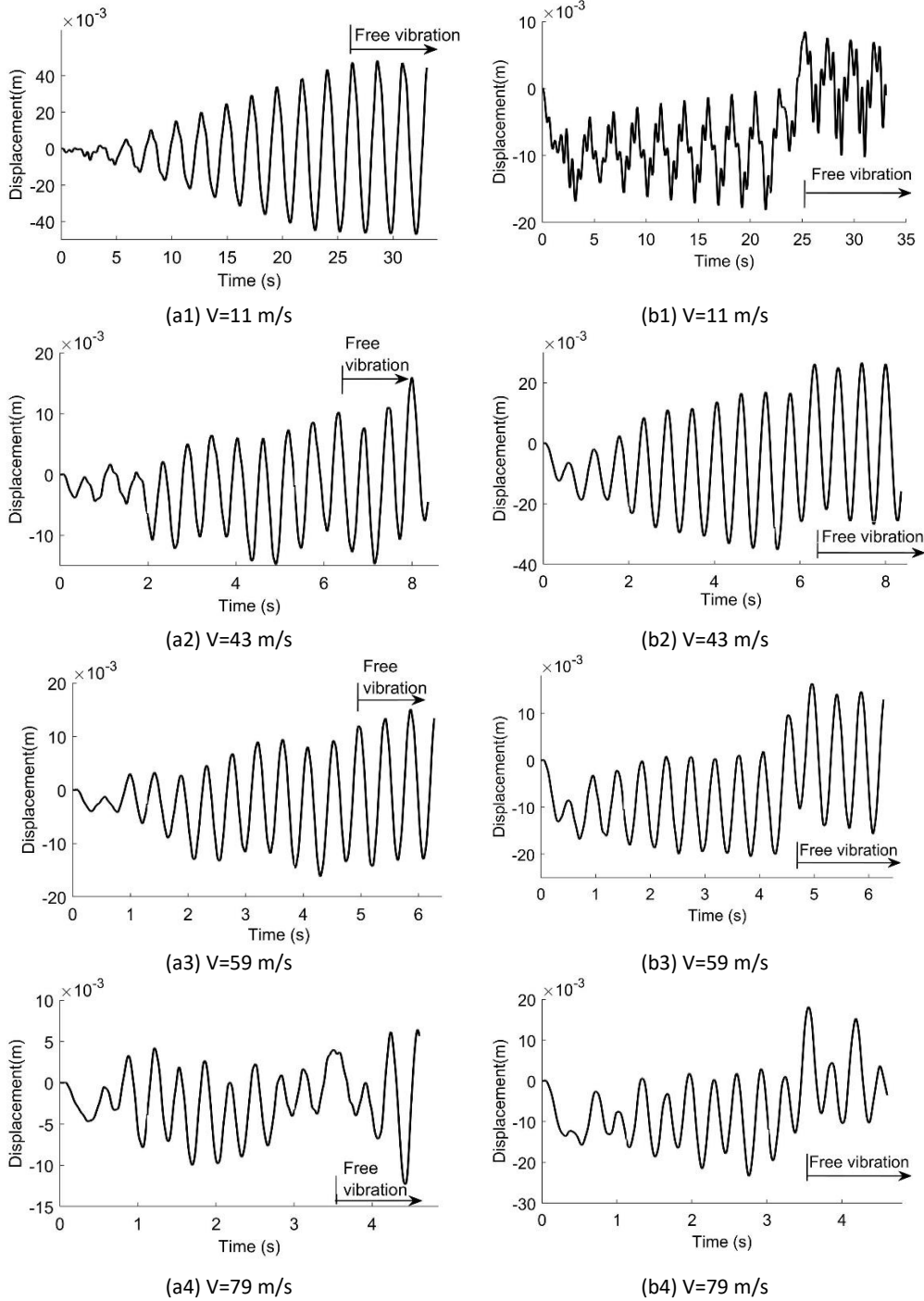


Figure 9: Figs. (ai) and (bi) (i=1,2,3) are corresponding to displacements at points p1 in the horizontal direction and p2 in the vertical directions, respectively

4. Conclusions

The study dealt with in this paper investigates effect of mode shapes on the dynamic response of the viaduct, based on the Bernoulli-Euler beam theory, subjected to train moving at velocity V . The various aspects of this work are:

- The first mode of the multi-bay frames is excited when the train is moving at low speed, etc. $V=11$ m/s = 39.6 km/h.
- The dominant modes are 1st and 2nd mode of 1-2 bay frames.
- The amplitude of the resonance vibrations decreased as the number of bays of the frame increased.
- Resonance vibrations were not encountered in the 3rd mode of the 1-bay frame, the 4th mode of the 2-bay frame, except for 1st mode of i -bay frame ($i=1,2$), where vertical displacements were negligible.

References

- [1] Su, D., Fujino, Y., Nagayama, T., Hernandez, J. Y., Seki, M. 2010. Vibration of reinforced concrete viaducts under high-speed train passage: Measurement and prediction including train-viaduct interaction, *Structures and Infrastructures Engineering*, vol. 6, no. 5, pp. 621–633, 2010, DOI: 10.1080/15732470903068888.
- [2] Lou, P., Dai, G. L., Zeng Q. Y. 2005. Modal coordinate formulation for a simply supported bridge subjected to a moving train modelled as two-stage suspension vehicles, *Proceedings of the Institution of Mechanical Engineers, Part C: Journal of Mechanical Engineering Science*, vol. 219, no. 10, pp. 1027–1040. DOI: 10.1243/095440605X31940.
- [3] Duan, Y. F., Wang, S. M., Wang, R. Z., Wang, C. Y., Shih, J. Y., Yun, C. B., 2018. Vector Form Intrinsic Finite-Element Analysis for Train and Bridge Dynamic Interaction, *Journal of Bridge Engineering*, vol. 23, no. 1, pp. 1–15. DOI: 10.1061/(ASCE)BE.1943-5592.0001171.
- [4] Hubbell, D., Gauvreau, P. 2018. Frequency Domain Analysis of Train – Guideway Interaction Dynamics, *Journal of Structural Engineering*, vol. 144, no. 8, pp. 1–11. DOI: 10.1055/s-0035-1570321.
- [5] Wu, Y. S., Yang, Y.-B. 2003. Steady-state response and riding comfort of trains moving over a series of simply supported bridges, *Engineering Structures*, vol. 25, no. 2, pp. 251–265. DOI: 10.1016/S0141-0296(02)00147-5.
- [6] Youcef, K., Sabiha, El Mostafa, T., D., Ali, D., Bachir, M. 2013. Dynamic analysis of train-bridge system and riding comfort of trains with rail irregularities, *Journal of Mechanical Science and Technology*, vol. 27, no. 4, pp. 951–962, DOI: 10.1007/s12206-013-0206-8.
- [7] Biondi, B., Muscolino, G., Sofi, A. 2005. A substructure approach for the dynamic analysis of train-track-bridge system, *Computers and Structures*, vol. 83, no. 28-30 SPEC. ISS, pp. 2271–2281. DOI: 10.1016/j.compstruc.2005.03.036.
- [8] Xiang, T., Zhao, R., Xu, T. 2007. Reliability Evaluation of Vehicle–Bridge Dynamic Interaction, *Journal of Structural Engineering*, vol. 133, no. 8, pp. 1092–1099, 2007. DOI: 10.1061/(ASCE)0733-9445(2007)133:8(1092).
- [9] Yang, Y.-B., Yau, J.-D., Hsu, L.-C. 1997. Vibration of simple beams due to trains moving at high speeds, *Engineering Structures*, vol. 19, no. 11, pp. 936–944. DOI: [http://dx.doi.org/10.1016/S0141-0296\(97\)00001-1](http://dx.doi.org/10.1016/S0141-0296(97)00001-1).
- [10] Lin, C. C., Wang, J. F., Chen, B. L. 2005. Train-Induced Vibration Control of High-Speed Railway Bridges Equipped with Multiple Tuned Mass Dampers, *Journal of Bridge Engineering*, vol. 10, no. 4, pp. 398–414. DOI: 10.1061/(ASCE)1084-0702(2005)10:4(398).
- [11] Demirtas, S., Ozturk, H., Sabuncu, M. 2019. Dynamic Response of Multi-bay Frames Subjected to Successive Moving Forces,” *International Journal of Structural Stability and Dynamics*, vol. 19, no. 4, pp. 1–24, DOI: 10.1142/S0219455419500421.
- [12] Bathe, K.-J. 1996 *Finite Element Procedures*. Prentice Hall, Upper Saddle River, New Jersey.
- [13] Yang, Y.-B., Chang, C., Yau, J. 1999. An Element for Analysing Vehicle Bridge Systems Considering Vehicle’s Pitching Effect, *International Journal for Numerical Methods in Engineering*, no. 46, pp. 1031–1047.

Appendix

In Eq. (7), the following abbreviations have been introduced:

$$\mathbf{M}_{fv}^i < q_1^{e_i} > = \begin{bmatrix} 0 \\ \cdot \\ \cdot \\ m_w N_1^2 \\ 0 \\ 0 \\ m_w N_1 N_2 \\ 0 \\ 0 \\ \cdot \\ 0 \end{bmatrix}$$

(A1)

$$\mathbf{M}_{fv}^i < q_4^{e_i} > = \begin{bmatrix} 0 \\ \cdot \\ \cdot \\ m_w N_1 N_2 \\ 0 \\ 0 \\ m_w N_2^2 \\ 0 \\ 0 \\ \cdot \\ 0 \end{bmatrix}$$

$$\mathbf{C}_{fv}^i < q_1^{e_i} > = \begin{bmatrix} 0 \\ \cdot \\ \cdot \\ 2Vm_w N_1 N_{1,x} + cN_1^2 \\ 0 \\ 0 \\ 2Vm_w N_{1,x} N_2 + cN_1 N_2 \\ 0 \\ 0 \\ \cdot \\ 0 \end{bmatrix} \tag{A2}$$

$$\mathbf{C}_{fv}^i < q_1^{e_i} > = \begin{bmatrix} 0 \\ \cdot \\ \cdot \\ 2Vm_w N_1 N_{2,x} + cN_1 N_2 \\ 0 \\ 0 \\ 2Vm_w N_2 N_{2,x} + cN_2^2 \\ 0 \\ 0 \\ \cdot \\ 0 \end{bmatrix}$$

$$\mathbf{K}_{fv}^i < q_1^{e_i} > = \begin{bmatrix} 0 \\ \cdot \\ \cdot \\ m_w V^2 N_1 N_{1,xx} + c V N_1 N_{1,x} + k N_1^2 \\ 0 \\ 0 \\ m_w V^2 N_1 N_{2,xx} + c V N_1 N_{2,x} + k N_1 N_2 \\ 0 \\ 0 \\ 0 \\ \cdot \\ \cdot \\ 0 \end{bmatrix}, \mathbf{K}_{fv}^i < q_4^{e_i} > = \begin{bmatrix} 0 \\ \cdot \\ \cdot \\ m_w V^2 N_{1,xx} N_2 + c V N_{1,x} N_2 + k N_1 N_2 \\ 0 \\ 0 \\ m_w V^2 N_2 N_{2,xx} + c V N_2 N_{2,x} + k N_2^2 \\ 0 \\ 0 \\ 0 \\ \cdot \\ \cdot \\ 0 \end{bmatrix} \quad (\text{A3})$$

where $\mathbf{A} < q_j^{e_i} >$ represents the j^{th} column of the element e_i in the matrix \mathbf{A} . Also,

$$\bar{\mathbf{A}}_{vf} = \begin{bmatrix} 0 & \dots & -aN_1 & 0 & 0 & -aN_2 & 0 & 0 & \dots & -aN_1 & 0 & 0 & -aN_2 & 0 & 0 & \dots & 0 \\ 0 & \dots & d_1 a N_1 & 0 & 0 & d_1 a N_2 & 0 & 0 & \dots & -d_2 a N_1 & 0 & 0 & -d_2 a N_2 & 0 & 0 & \dots & 0 \end{bmatrix}^T, \quad (\text{A4})$$

$$\bar{\mathbf{A}}_v = \begin{bmatrix} 2a & (d_2 - d_1)a \\ (d_2 - d_1)a & (d_1^2 + d_2^2)a \end{bmatrix}$$

$$\mathbf{f} = [0 \quad \cdot \quad f_1^{e_i} \quad 0 \quad 0 \quad f_4^{e_i} \quad 0 \quad 0 \quad \cdot \quad 0]^T \quad (\text{A5})$$

where $i=1,2$. $f_1^{e_i}$ and $f_4^{e_i}$ represent the vehicle loads exerted by each wheelset on the contacting element i and those are determined as follows:

$$f_1^{e_i} = - \left(m_w + m_v \frac{d_2}{d_1 + d_2} \right) g N_1 \quad (\text{A6})$$

$$f_4^{e_i} = - \left(m_w + m_v \frac{d_1}{d_1 + d_2} \right) g N_2$$

where g is the acceleration due to gravity.

If \mathbf{A} and a in matrices $\bar{\mathbf{A}}_{vf}$ and $\bar{\mathbf{A}}_v$ in Eq. (A5) are replaced by \mathbf{C} and c (or \mathbf{K} and k), matrices $\bar{\mathbf{C}}_{vf}$ and $\bar{\mathbf{C}}_v$ (or matrices $\bar{\mathbf{K}}_{vf}$ and $\bar{\mathbf{K}}_v$) can be determined.